JOURNAL OF Applied Polymer SCIENCE

Role of dual dopants in highly ordered crystalline polyaniline nanospheres: Electrode materials in supercapacitors

Rajender Boddula, Palaniappan Srinivasan
Polymers and Functional Materials Division, Indian Institute of Chemical Technology, Council of Scientific and Industrial Research, Hyderabad 500 007, India
Correspondence to: S. Palaniappan (E-mail: palani74@rediffmail.com)

ABSTRACT: Aniline is oxidized by ammonium persulfate oxidant with a weak organic acid, 1,3-(6,7)-napthalene trisulfonic acid (NTSA), via an aqueous polymerization pathway to polyaniline (PANI) salt. The effects of the sodium lauryl sulfate surfactant, mineral acid [sulfuric acid (H_2SO_4)], and a combination of surfactant with mineral acid in the aniline polymerization reaction are also carried. These salts were designated as PANI–NTSA–dodecyl hydrogen sulfate (DHS), PANI–NTSA–H_2SO_4, and PANI–NTSA–DHS–H_2SO_4, respectively. Interestingly, PANI–NTSA–DHS showed a highly ordered crystalline sample with a nanosphere morphology. These PANIs were used as electrode materials in supercapacitor applications. Among the four salts, the PANI–NTSA–DHS–H_2SO_4 material showed higher values of specific capacitance (520 F/g), energy (26 W h/kg), and power densities (200 W/kg) at 0.3 A/g. Moreover, 77% of the original capacitance was retained after 2000 galvanostatic charge–discharge cycles with a Coulombic efficiency of 98–100%. PANI–NTSA–DHS–H_2SO_4 was obtained in excellent yield with an excellent conductivity (6.8 S/cm) and a thermal stability up to 235°C. © 2015 Wiley Periodicals, Inc. J. Appl. Polym. Sci. **2015**, *132*, 42510.

KEYWORDS: applications; conducting polymers; electrochemistry; nanostructured polymers

accepted 16 May 2015
DOI: 10.1002/app.42510

INTRODUCTION

Electrochemical capacitors, also called *supercapacitors* or *ultracapacitors,* are promising energy-storage devices because of their advantages, which include a high-power capability and longer cycle life, and because they are maintenance-free devices.[1–3] The performances of supercapacitors are primarily determined by active electrode materials based on carbon,[4] metal oxides,[5] and conducting polymers.[6–15] Among the conducting polymers, polyaniline (PANI) salt has been regarded as one of the most promising supercapacitor electrode materials because of its low cost, easy synthesis, larger pseudo-capacitance, faster doping–dedoping rate during the charge–discharge (CD) process, low toxicity, and good environmental stability.[7] Literature reports on the electrochemical performances of PANIs in an aqueous sulfuric acid (H_2SO_4) electrolyte as single electrode or in cell configuration are given in Table I.

In this study, 1,3-(6,7)-napthalene trisulfonic acid trisodium salt (NTSA–Na) was used as a dopant for the preparation of PANI salt via an aqueous polymerization pathway by the oxidation of aniline with ammonium persulfate. In the course of polymerization, NTSA–Na got converted into naphthalene trisulfonic acid (NTSA) under acidic conditions and was incorporated into the PANI system. In addition to NTSA–Na, the effect of the surfactant [sodium lauryl sulfate (SLS)], mineral acid (H_2SO_4), and mixture of surfactant and mineral acid in the preparation of PANI salts were also carried out (Scheme 1). These PANI–NTSA samples were used as electrode materials in supercapacitor applications, and we evaluated their performances.

EXPERIMENTAL

Materials

NTSA–Na (Sigma Aldrich), 98% H_2SO_4 (Laboratory Reagent, Merck, India), ammonium persulfate, SLS (S.D. Fine Chemicals, India), and other reagents were all analytical-reagent grade and were used without further treatment. Aniline (analytical-reagent grade, Rankem, India) was distilled before use. Distilled water was used throughout this study.

Preparation of PANI–NTSA

Aniline (0.93 g, 0.1*M*) and NTSA–Na hydrate (4.34 g, 0.1*M*) were dissolved in 50 mL of distilled water. To this solution, 50 mL of distilled water containing ammonium persulfate (2.28 g, 0.1*M*) was added as a whole. The mixture was stirred constantly for 4 h at ambient temperature. The green precipitate was filtered, washed several times with distilled water followed by acetone. The powder sample was dried at 50°C in an oven until a constant weight was reached.

Table I. Literature Report on PANI-Based Supercapacitor Systems

System	C/EC	Configuration	CV/CD	Voltage range	*Cs* (F/g)	*E* (W h/kg)	*P* (W/kg)	Reference
PANI-HCl	C	Electrode	CD	0.0–0.7	548	36	127	8
PANI-HCl	C	Electrode	CD	−0.2 to 0.8	232	32	200	9
PANI-citrate	C	Electrode	CV	−0.2 to 1.0	298	—	—	10
PANI-H_2SO_4	EC	Cell	CV	0.0–0.6	230	4.25	1200	11
PANI-H_2SO_4	EC	Electrode	CD	0.0–0.6	180	—	—	12
PANI-H_2SO_4	EC	Cell	CD	0.0–0.8	70			13
PANI-$LiPF_6$	C	—	CD	0.0–1.0	168	—	—	14
PANI-H_2SO_4	EC	Electrode	CV	0.0–0.75	486	—	—	15
PANI-NTSA	C	Cell	CD	0.0–0.6	520	26	200	This study

C, chemical synthesis; *Cs*, specific capacitance; EC, electrochemical synthesis.

Preparation of PANI–NTSA–Dodecyl Hydrogen Sulfate (DHS)
In the previous reaction (PANI–NTSA), SLS (1 g, 0.035*M*) was placed, along with aniline and NTSA–Na hydrate, in 50 mL of water, and the polymer sample was isolated by the same procedure.

Preparation of PANI–NTSA–H_2SO_4
In the previous reaction (PANI–NTSA), aqueous H_2SO_4 (1*M*) was placed, along with aniline and NTSA–Na hydrate, in 50 mL of water, and the polymer sample was isolated by the same procedure.

Preparation of PANI–NTSA–DHS–H_2SO_4
In the previous reaction (PANI–NTSA), SLS (1 g, 0.035*M*) and aqueous H_2SO_4 (1*M*) were placed, along with aniline and NTSA–Na hydrate, in 50 mL of water, and the polymer sample was isolated by the same procedure.

Characterization
Powder of PANI was pressed into a disk 13 mm in diameter and about 1.5 mm in thickness under a pressure of 120 kg/cm^2. The resistance of the pellet was measured by a four-probe method with a Keithley constant source (model 6220) and nanovoltmeter (model 2182A, Keithley, Cleveland, OH). The pellet density was measured from the mass per unit volume of the pressed pellet. Fourier transform IR spectra of the polymer samples were registered on a Fourier transform IR spectrometer (Thermo Nicolet Nexus 670) with KBr pressed-pellet technique. X-ray diffraction (XRD) profiles for the polymer powders were obtained on a Siemens/D-500 X-ray diffractometer with Cu Kα radiation and scan speed of 0.045°/min. Morphological studies (microstructural and elemental analysis) of the polymer samples were performed via field emission scanning electron microscopy (FESEM) with a Hitachi S-4300 instrument (Tokyo, Japan). The sample was mounted on a carbon disc with the help of double-sided adhesive tape and sputter-coated with a thin layer of gold to prevent sample-charging problems. The electrochemical performances of all of the PANI samples were investigated with two-electrode Swagelok-type cells without a reference electrode. The PANI–NTSA electrode was made through the pressing of

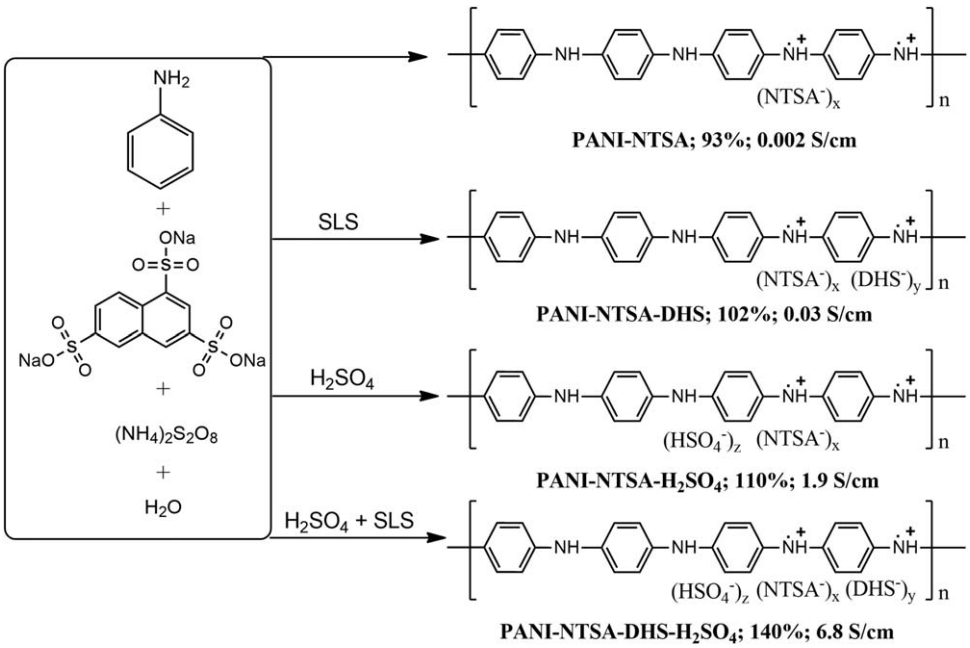

Scheme 1. Synthesis of PANIs via an aqueous polymerization pathway.

3 mg of the PANI sample on stainless steel mesh by the application of 100 kg/cm^2 of pressure. Two electrodes with identical samples were assembled for a supercapacitor cell with an aqueous 1*M* H_2SO_4 electrolyte solution. Cyclic voltammetry (CV) and galvanostatic CD experiments were carried out with a WonATech multichannel potentiostat–galvanostat (WMPG1000, GyeongGi-Do, Korea). Cyclic voltammograms were recorded from −0.2 to 0.6 V at various sweep rates, and galvanostatic CD experiments were carried out from 0 to 0.6 V. Electrochemical impedance spectroscopy (EIS) measurements were carried out with an IM6ex Zahner-Elektrik instrument (Germany) in the frequency (*f*) range 40 kHz–10 mHz at various voltages with a three-electrode cell configuration, that is, with PANI salt as the working electrode, a platinum counter electrode, and a saturated calomel electrode as a reference electrode. All of the electrochemical measurements were carried out at ambient temperature.

The specific capacitance from cyclic voltammetry (CV-*Cs*) was calculated with the following formula:

$$CV-Cs=\frac{Q\times 1000}{\Delta Vm}$$

where Q is the total voltammetric charge, ΔV is the voltage window, and m is the mass of one electrode.

The discharge-specific capacitance (CD-C_s), energy density (E), and power density (P) from the galvanostatic CD experiment were calculated from the following formula:

$$\mathrm{CD}-Cs=2\frac{I\Delta t}{\Delta Vm}$$

$$E=\frac{\Delta VI\Delta t}{m}$$

$$P=\frac{\Delta VI}{m}$$

where I is the charge–discharge current and Δt is the discharge time.

The amount of drop is a function of the equivalent series resistance (ESR) and *I*, as indicated by the following equation:

$$\mathrm{ESR}\ =dV/I$$

where dV is the voltage drop.

The Coulombic efficiencies (η) of the supercapacitor were calculated with the following formula:

$$\eta=\frac{tD}{tC}\times 100$$

where t_D is the expression for discharge time and t_C is the expression for charge time.

Specific capacitance from electrochemical impedance spectroscopy (EIS-C_s) is calculated with the following formula:

$$\mathrm{EIS}-Cs=\frac{-1}{2\pi fZ_{im}m}$$

where Z_{im} is the impedance of the imaginary part (Ω).

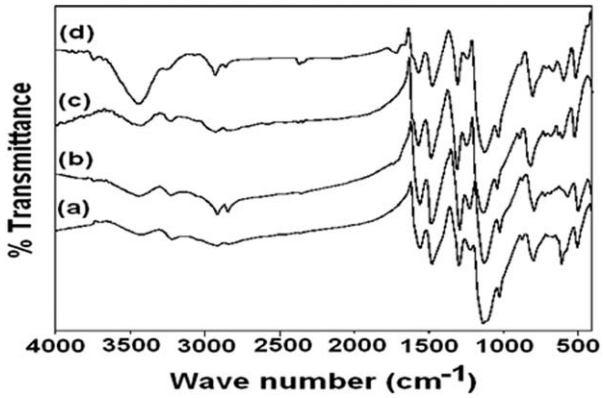

Figure 1. Fourier transform IR spectra of (a) PANI–NTSA, (b) PANI–NTSA–DHS, (c) PANI–NTSA–H_2SO_4, and (d) PANI–NTSA–DHS–H_2SO_4.

RESULTS AND DISCUSSION

The value of the yield and conductivity for the PANI salts are reported in Scheme 1. Because the PANIs were not soluble in common organic solvents, no efforts were made to determine the molecular weight of the polymer. Hence, the yield of the PANIs are represented as percentages; these values were calculated with respect to the amount of aniline used in the reaction. The values of the yield and conductivity of PANI–NTSA were 0.93 g and 0.002 S/cm, respectively. The values of the yield and conductivity increased with the use of surfactant and then further increased with the use of mineral acid; they still further increased with the use of the surfactant–mineral acid mixture. This result indicates that the oxidizing and doping power increased with the use of surfactant and inorganic acid. The formation of PANI salts containing sulfonic acid groups was confirmed from the IR spectra.

The IR spectra of the PANI–NTSA salts are shown in Figure 1. The IR spectra of all four salts were greater or similar, and they showed major characteristic peaks of PANI salt[16–18] at 3440–3445 cm^{-1} (N—H stretching), 3220–3225 cm^{-1} (NH^+, indicative of doping, i.e., salt formation), 2920–2925 cm^{-1} (C—H stretching), 1560–1565 cm^{-1} (C═C stretching, quinonoid ring), 1465–1490 cm^{-1} (C═C stretching, benzenoid ring), 1300 cm^{-1} (C—N stretching, quinonoid ring), 1225–1240 cm^{-1} (C—N stretching, benzenoid ring), 1120–1140 cm^{-1} (N═Q═N vibrations, where Q represents the quinonoid ring), and 800 cm^{-1} (1,4-disubstituted benzene). In addition, the peaks at 1030 and 505 cm^{-1} were assigned to the asymmetric and symmetric O═S═O stretching vibrations, and the peak at 640 cm^{-1}, attributable to the C—S stretching vibrations; this denoted the existence of an SO_3^- group.[17] In the case of PANI–NTSA–DHS–H_2SO_4, the IR spectrum [Figure (1d)] showed an additional peak at 1710 cm^{-1} because of the C═O bond. This peak indicated that PANI salt underwent overoxidation, which resulted the formation of C═O bonds. This overoxidation was due to the higher efficiency of oxidation of aniline by the use of NTSA along with SLS and H_2SO_4.

The XRD patterns of the four PANI salts are shown in Figure 2. The PANI–NTSA showed four clear peaks around 2θ values of 16, 20, 25, and 27° with corresponding *d*-spacings of 6.0, 4.5,

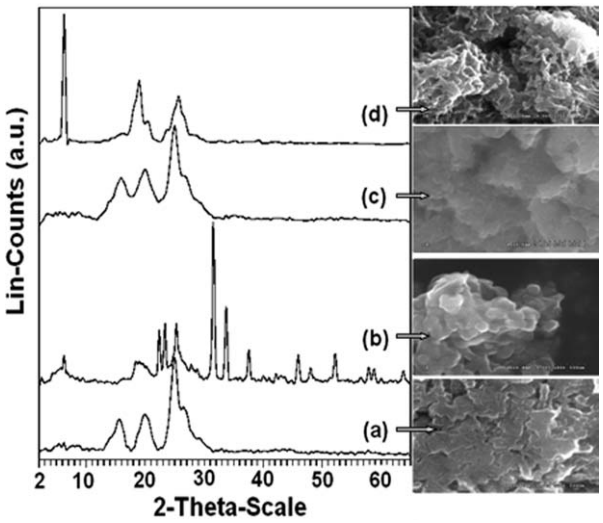

Figure 2. XRD patterns with corresponding FESEM images of (a) PANI–NTSA, (b) PANI–NTSA–DHS, (c) PANI–NTSA–H_2SO_4, and (d) PANI–NTSA–DHS–H_2SO_4.

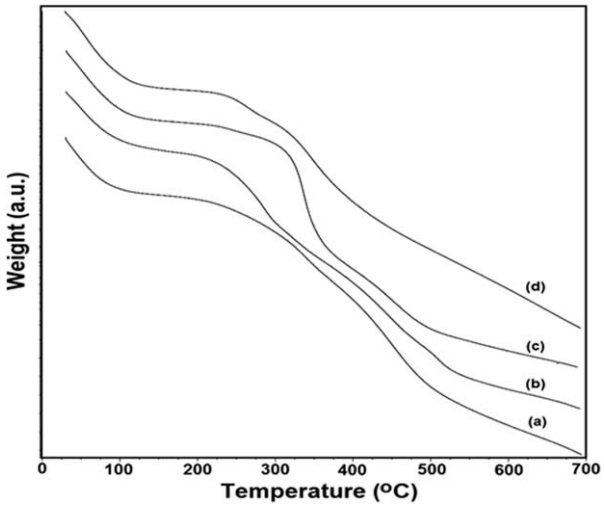

Figure 3. Thermograms of PANI: (a) PANI–NTSA, (b) PANI–NTSA–DHS, (c) PANI–NTSA–H_2SO_4, and (d) PANI–NTSA–DHS–H_2SO_4.

3.5, and 3.3Å, respectively [Figure (2a)]. Generally, the XRD pattern of the emeraldine from the PANI salt showed peaks at 9.3, 15, 22, and 27 with a shoulder at 29°; this corresponded to a semicrystalline nature.[19] Thus, the XRD pattern of PANI–NTSA indicated the formation of a semicrystalline form of PANI. However, surprisingly, on the addition of SLS to the reaction, the PANI–NTSA–DHS salt, showed bands at 6.1°, 19° (broad), 22°, 23°, 25°, 31°, 34°, and 38° (very intense, sharp), 46°, 48°, 52°, 58°, and 59° (intense sharp), with corresponding *d*-spacings of 14.4, 4.44, 3.99, 3.82, 3.53, 2.84, 2.66, 2.39, 1.97, 1.89, 1.75, 1.59, and 1.57 Å [Figure (2b)]. The observation of many intense sharp peaks in addition to the PANI salt peaks in the higher angle region indicated the formation of a highly ordered PANI salt. The peak at a lower angle of $2\theta = 6.1°$ was due to the presence of a surfactant moiety,[20] and this result indicated that in the course of polymerization, SLS got converted into DHS under the acidic conditions and incorporated into the PANI system.[18] On the addition of mineral acid along with NTSA–Na, the reaction gave PANI–NTSA–H_2SO_4 [Figure (2c)] with a similar XRD pattern of PANI–NTSA with a small shift in the positions (15.6, 19.7, 24.6, and 26.3°). On addition of both surfactant and mineral acid, the XRD pattern of PANI–NTSA–DHS–H_2SO_4 [Figure (2d)] showed a similar XRD pattern of PANI–NTSA along with a sharp lower angle peak at $2\theta = 6.3°$ due to the long-range ordering of PANI chains via the doping of the surfactant molecules.[20]

FESEM images of the four PANIs are included in Figure 2. The FESEM image of PANI–NTSA showed a spongelike morphology [Figure (2a)]; the addition of surfactant (SLS) to the reaction led to the formation of a nanosphere morphology [diameter range = 110–240 nm; Figure (2b)], the addition of mineral acid, morphological changes with a flakelike morphology [Figure (2c); PANI–NTSA–H_2SO_4], and the addition of both the mineral acid and surfactant led to the formation of a nanofiber morphology [PANI–NTSA–DHS–H_2SO_4; Figure (2d)]. This observation indicated that the morphology of PANIs varied with the synthetic methods.

The previous results indicate that the use of NTSA–Na in the oxidation of aniline led to the formation of a semicrystalline PANI salt with a spongelike morphology, wherein NTSA acted as a weak protonating agent for the PANI salt. The use of the SLS surfactant along NTSA–Na led to the formation of a highly ordered crystalline nanosphere form of PANI salt containing the dual dopants, DHS and NTSA. However, the use of a strong acid H_2SO_4 along with NTSA–Na, led to a flakelike morphology of semicrystalline PANI salts containing NTSA and strong H_2SO_4 dopants. The use of SLS and H_2SO_4 led to overoxidized PANIs with a semicrystalline nature.

The thermal stability of the PANIs were measured by the subjection of PANIs for thermogravimetric analysis (Figure 3). Thermogravimetric analysis indicated that the PANIs contained moisture, and the stability of the salts were in the following order: PANI–NTSA–H_2SO_4 (300°C) > PANI–NTSA–DHS–H_2SO_4 (235°C) > PANI–

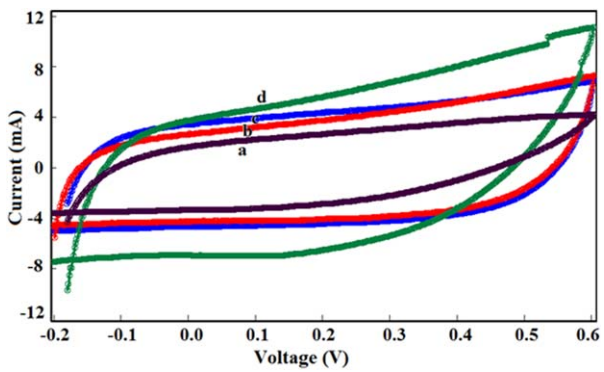

Figure 4. CV curves of the (a) PANI–NTSA, (b) PANI–NTSA–DHS, (c) PANI–NTSA–H_2SO_4, and (d) PANI–NTSA–DHS–H_2SO_4 electrodes at a scanning rate of 10 mV/s. [Color figure can be viewed in the online issue, which is available at wileyonlinelibrary.com.]

Table II. Electrochemical Parameters for the PANI Samples Obtained from the CV and CD Studies

Sample	CV-*Cs* at 10 mV/s (F/g)	CD at current density of 0.3 A/g		
		CD-*Cs* (F/g)	*E* (W h/kg)	*P* (W/kg)
PANI-NTSA	300	444	22.2	200
PANI-NTSA-DHS	244	470	23.5	200
PANI-NTSA-H_2SO_4	280	500	25.0	200
PANI-NTSA-DHS-H_2SO_4	380	520	26.0	200

NTSA–DHS (220°C) > PANI–NTSA (205°C). PANIs underwent degradation past the thermal stability temperature. The moisture content for the PANI–NTSA–DHS–H_2SO_4 sample, and this was confirmed from the heat-treatment study. The moisture present in the PANIs was calculated by the subjection of the PANI samples to heat treatment at 110°C. The weight loss of the sample was found from the initial and final weights of the samples. The experiments showed a weight loss of around 15%.

In this study, the PANI–NTSA salts were explored as electrode materials in supercapacitor applications. The electrochemical performance of the PANI–NTSA samples was carried out by CV (Figure 4). The CV pattern showed an almost rectangular shape, which revealed excellent capacitive behavior. This result implies that the diffusion of ions from the electrolyte could gain access to almost all of the available pores of the electrode. The CV-*Cs* values were calculated from the CV curve. CV-*Cs* was calculated with respect to *m*. As a representative system, the value of CV-*Cs* calculated at a higher scan rate (10 mV/s) for the sample PANI–NTSA–DHS–H_2SO_4 (380 F/g) was found to be higher than that of the samples PANI–NTSA (300 F/g), PANI–NTSA–DHS (244 F/g), and PANI–NTSA–H_2SO_4 (280 F/g; Table II).

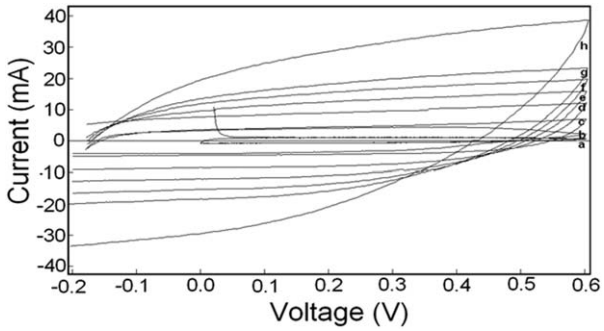

Figure 5. CV curves of the PANI–NTSA–DHS–H_2SO_4 electrode at scanning rates of (a) 1, (b) 5, (c) 10, (d) 20, (e) 30, (f) 40, (g) 50, and (h) 100 mV/s.

CV of the cell with the use of the PANI–NTSA–DHS–H_2SO_4 material was measured at various scan rates (1, 5, 10, 20, 30, 40, 50, and 100 mV/s), and the corresponding CV-*Cs* values were found to be 520, 488, 380, 284, 254, 234, 218, and 150 F/g, respectively (Figure 5). A very important observation was that the curves at different scan rates showed no peaks; this indicated that the electrode was charged and discharged at a pseudo constant rate over the complete CV cycle or implied very rapid and reversible electrochemical processes. Another observation was that even with the very high scan rate at 100 mV/s, the shape of the CV curve was still maintained, and this demonstrated the high performance of the supercapacitor.

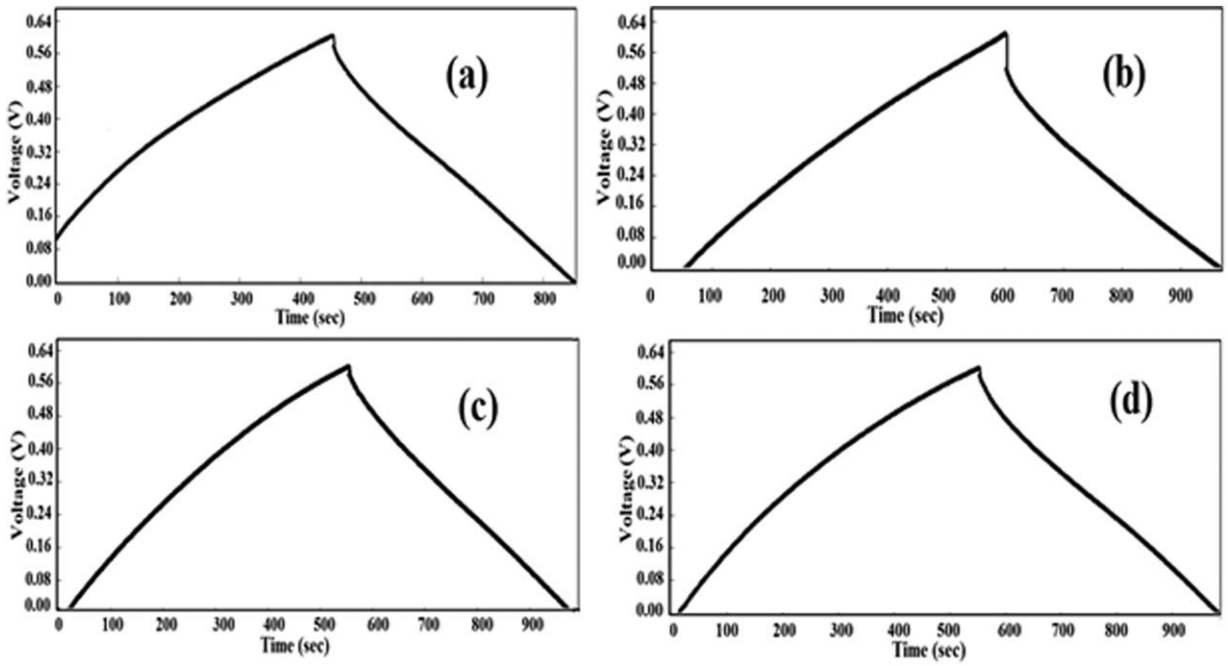

Figure 6. CD cycling of the (a) PANI–NTSA, (b) PANI–NTSA–DHS, (c) PANI–NTSA–H_2SO_4, and (d) PANI–NTSA–DHS–H_2SO_4 electrodes at a current density of 0.3 A/g.

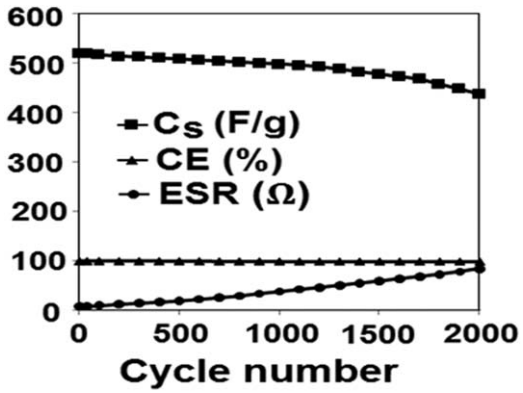

Figure 7. Capacitance, ESR, and η (CEs) with cycle numbers at a current density of 0.3 A/g for PANI–NTSA–DHS–H_2SO_4.

CD behavior is an important characteristic for the practical application of supercapacitors. As representative systems, the value of CD-*Cs* at a current density of 0.3 A/g (Table II) for the sample PANI–NTSA–DHS–H_2SO_4 (520 F/g) was found to be higher that of the samples PANI–NTSA–H_2SO_4 (500 F/g), PANI–NTSA–DHS (470 F/g), and PANI–NTSA (444 F/g; Figure 6). We achieved a high capacitance value of 520 F/g for PANI (PANI–NTSA–H_2SO_4–DHS) compared to that of the other PANIs carried in a symmetric cell configuration (Table I).

All four PANI salts showed a similar value of energy (23–26 W h/kg) and *P*s (200 W/kg, Table II). For practical applications, the supercapacitor must have long-term cycle stability. Among the four PANI salts, PANI–NTSA–DHS–H_2SO_4 showed a higher capacitance, and hence, the PANI–NTSA–DHS–H_2SO_4 cell was subjected to CD cycles (up to 2000 cycles) at a current density of 0.3 A/g. The capacitance, η, and ESR values with 2000 cycles are shown in Figure 7. The retention in the value of CD-*Cs* at 2000 cycles was found to be 77% with its initial capacitance value of 520 F/g. The ηs were found to be constant with cycle number (98–100%). The ESR value increased from 8.1 to 85 Ω at the end of 2000 cycles. The increase in the ESR value indicated that the PANI salt underwent deterioration because of the fast doping and dedoping process with CD cycles.

EIS is an important analytical technique that is used to gain information about the characteristic *f* responses of the supercapacitors and the capacitive phenomena occurring in the electrodes. The impedance spectra for the four PANI salts were obtain with an applied voltage of 0.6 V, and the plots of *f* versus capacitance are shown in Figure 8. The value of EIS-*Cs* obtained at 10-mHz *f* for PANI–NTSA–DHS–H_2SO_4 (320 F/g) was found to be higher that of the samples PANI–NTSA (270 F/g), PANI–NTSA–H_2SO_4 (225 F/g), and PANI–NTSA–DHS (195 F/g). Low values of solution resistance (R_s), charge-transfer resistance (R_{ct}), and time constant (τ) were observed for PANI–NTSA–H_2SO_4 (Table III), and this result signposted the fast CD behavior during the CD cycles.

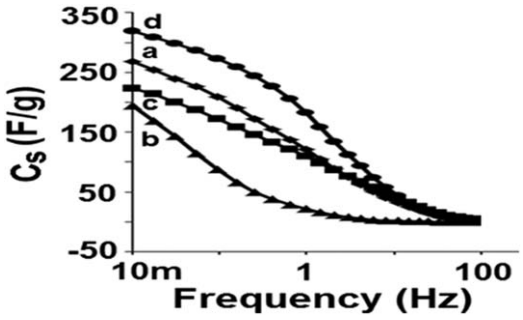

Figure 8. *f* versus EIS-Cs in the range of 40 kHz to 100 Hz at a potential of 0.6 V for (a) PANI–NTSA, (b) PANI–NTSA–DHS, (c) PANI–NTSA–H_2SO_4, and (d) PANI–NTSA–DHS–H_2SO_4.

Table III. R_s, R_{ct}, τ, and EIS-*Cs* Values for the PANI Salts at 0.6 V from the Impedance Measurements

Sample	R_s (Ω)	R_{ct} (Ω)	τ (ms)	EIS-*Cs* (F/g)
PANI-NTSA	0.89	0.99	0.38	270
PANI-NTSA-DHS	0.83	10.7	3.50	195
PANI-NTSA-H_2SO_4	0.86	0.83	0.31	225
PANI-NTSA-DHS-H_2SO_4	1.34	1.48	0.48	320

The operating *f* (the *f* at which the capacitance was at 50% of its maximum value) was observed to be close to 1 Hz for and PANI–NTSA–DHS–H_2SO_4 and PANI–NTSA–H_2SO_4, and small lower operating *f*s were observed for PANI–NTSA (0.6 Hz) and PANI–NTSA–DHS (0.2 Hz).

CONCLUSIONS

In summary, PANI containing a weak organic acid, 1,3-(6,7)-napthalene trisulfonic acid (NTSA), was synthesized by an aqueous polymerization pathway. The effect of the surfactant, mineral acid, and a combination of both the surfactant and mineral acid in the formation of PANIs were also carried out. This study showed that the use of a surfactant along with a weak organic acid containing sodium salt in the oxidation of aniline led to the formation of a highly ordered crystalline PANI having a nanosphere morphology. Moreover, PANI was obtained with excellent yield and conductivity and a high electrochemical performance.

ACKNOWLEDGMENTS

The authors thank the Department of Science of Technology of New Delhi for funding through project DST/TSG/PT/2011/179-G. They also thank Vijayamohanan K. Pillai, Director of the Central Electro Chemical Research Institute (Council of Scientific and Industrial Research), Karaikudi, for his valuable discussion. Boddula Rajender is thankful to the University Grants Commission of India for its financial assistance.

REFERENCES

1. Miller, J. R.; Outlaw, R. A.; Holloway, B. C. *Science* **2010**, *329*, 1637.
2. Ji, H. X.; Zhao, X.; Qiao, Z. H.; Jung, J.; Zhu, Y. W.; Lu, Y. L.; Zhang, L. L.; MacDonald, A. H.; Ruoff, R. S. *Nat. Commun.* **2014**, *5*, 3317.

3. Bo, Z.; Zhu, W. G.; Ma, W.; Wen, Z. H.; Shuai, X. R.; Chen, J. H.; Yan, J. H.; Wang, Z. H.; Cen, K. F.; Feng, X. L. *Adv. Mater.* **2013**, *25*, 5799.
4. Frackowiak, E.; Beguin, F. *Carbon* **2001**, *39*, 937.
5. Deng, W.; Ji, X.; Chen, Q.; Banks, C. E. *RSC Adv.* **2011**, *1*, 1171.
6. Snook, G. A.; Kao, P.; Best, A. S. *J. Power Sources* **2011**, *196*, 1.
7. Bhadra, S.; Khastgir, D.; Singha, N. K.; Lee, J. H. *Prog. Polym. Sci.* **2009**, *34*, 783.
8. Guan, H.; Fan, L. Z.; Zhang, H. C.; Qu, X. H. *Electrochim. Acta* **2010**, *56*, 964.
9. Dai, T.; Jia, Y. *Polymer* **2011**, *52*, 2550.
10. Subramania, A.; Devi, S. L. *Polym. Adv. Tech.* **2008**, *19*, 725.
11. Talbi, H.; Just, P.; Dao, L. *J. Appl. Electrochem.* **2003**, *33*, 465.
12. Chen, W. C.; Wen, T. C.; Teng, H. S. *Electrochim. Acta* **2003**, *48*, 641.
13. Tamai, H.; Hakoda, M.; Shiono, T.; Yasuda, H. *J. Mater. Sci.* **2007**, *42*, 1293.
14. Ryu, K. S.; Wu, X. L.; Lee, Y. G.; Chang, S. H. *J. Appl. Polym. Sci.* **2003**, *89*, 1300.
15. Sumboja, A.; Tefashe, U. M.; Wittstock, G.; Lee, P. S. *Adv. Mater. Interfaces* **2015**, *2*, 1400154.
16. Palaniappan, S.; Rajender, B. *Adv. Synth. Catal.* **2010**, *352*, 2507.
17. Khalid, M.; Tumelero, M. A.; Brandt, I. S.; Zoldan, V. C.; Acuña, J. J. S.; Pasa, A. A. *Indian J. Mater. Sci.* **2013**, *2013*, 718304.
18. Palaniappan, S.; Lakshmi Devi, S. *J. Appl. Polym. Sci.* **2008**, *107*, 1887.
19. Pouget, J. P.; Jdzefowiczt, M. E.; Epstein, A. J.; Tang, X.; MacDiarmid, A. G. *Macromolecules* **1991**, *24*, 779.
20. Antony, M. J.; Jayakannan, M. *J. Phys. Chem. B* **2010**, *114*, 1314.